Biointerphases
A Journal of Biomaterials and Biological Interfaces

Evaluation of a biomimetic poly(ε-caprolactone)/β-tricalcium phosphate multispiral scaffold for bone tissue engineering: *In vitro* and *in vivo* studies

Cite as: Biointerphases **9**, 029011 (2014); https://doi.org/10.1116/1.4870781
Submitted: 20 January 2014 • Accepted: 28 March 2014 • Published Online: 09 April 2014

Esra Baykan, Aysel Koc, Ayse Eser Elcin, et al.

View Online Export Citation CrossMark

ARTICLES YOU MAY BE INTERESTED IN

The rationale and emergence of electroconductive biomaterial scaffolds in cardiac tissue engineering
APL Bioengineering **3**, 041501 (2019); https://doi.org/10.1063/1.5116579

Accelerated Escherichia coli inactivation in the dark on uniform copper flexible surfaces
Biointerphases **9**, 029012 (2014); https://doi.org/10.1116/1.4870596

On the long term antibacterial features of silver-doped diamondlike carbon coatings deposited via a hybrid plasma process
Biointerphases **9**, 029013 (2014); https://doi.org/10.1116/1.4871435

AVS Quantum Science
Now Publishing Original Research
Co-Published by AIP Publishing AVS
LEARN MORE

© 2014 American Vacuum Society.

Evaluation of a biomimetic poly(ε-caprolactone)/β-tricalcium phosphate multispiral scaffold for bone tissue engineering: *In vitro* and *in vivo* studies

Esra Baykan, Aysel Koc, Ayse Eser Elcin, and Yasar Murat Elcin[a)]
Tissue Engineering, Biomaterials and Nanobiotechnology Laboratory, Ankara University Faculty of Science and Ankara University Stem Cell Institute, Ankara 06100, Turkey

(Received 20 January 2014; accepted 28 March 2014; published 9 April 2014)

In this study, the osteogenic potential of rat bone marrow mesenchymal stem cells (rBM-MSCs) on a biomimetic poly(ε-caprolactone)/β-tricalcium phosphate (PCL/β-TCP) composite scaffold composed of parallel concentric fibrous membranes was evaluated *in vitro* and *in vivo*. PCL/β-TCP composite membranes were prepared by electrospinning and characterized by x-ray diffraction, differential scanning calorimetry, Fourier transform-infrared spectroscopy, and scanning electron microscopy (SEM). rBM-MSCs were seeded on three-dimensional multispiral scaffolds prepared by the assembly of composite membranes. The cell-scaffold constructs were cultured in osteogenic medium for 4 weeks. Histochemical studies and biochemical assays confirmed the osteogenic differentiation of rBM-MSCs inside the scaffold by documenting the dense mineralized extracellular matrix formation starting from the second week of culture. In the *in vivo* part of the study, cell-scaffold constructs precultured for 7 days were implanted subcutaneously into the epigastric groin fascia of Wistar rats for a duration of 6 months. Ectopic bone-tissue like formation was documented by using computerized tomography, confocal laser microscopy, SEM, and histochemistry. *In vivo* findings indicated that the biomimetic multispiral scaffold seeded with rBM-MSCs supports the ectopic formation of new bone tissue in Wistar rats. © *2014 American Vacuum Society*.
[http://dx.doi.org/10.1116/1.4870781]

I. INTRODUCTION

Bone damage can be caused by an array of reasons such as trauma and tumor resection. Musculoskeletal tissues, particularly bone, is the most widely transplanted tissue in orthopedic surgery. Defect size, location, and mechanical stresses show great variation, so the surgical solution has to be versatile. For successful bone repair, epiphyses should get closer and the gap in between should be filled with implant materials.[1] Reconstructive procedures of bone are usually undertaken with conventional, noncellular permanent materials. Although autograft implants are qualified as gold standard for healing bone defects, donor site scarcity and limited number of donors are still important problems.[2–4] Use of allografts has considerable drawbacks such as the risk of immune rejection and pathogen transfer. To eliminate immunogenic proteins, bone grafts have to undergo processes such as irradiation, freeze-drying, and lyophilization. Bone-mimetic biomaterials emerge as an alternative to existing treatment methods.[5,6] Bone tissue engineering involves implantation of scaffolds on the damaged bone section. These scaffolds are seeded with donor cells proliferated *in vitro*.[7,8] As a basic concept, biomimetic scaffolds for bone tissue engineering must favor biological functions such as cell adherence, proliferation, and differentiation. New bone tissue formation promotes graft stability and improves bone function.[9,10]

There are several techniques used for the fabrication of biomaterials that replace and repair damaged or traumatized bone tissues.[2] Intended structure can be built through various methods such as electrospinning, particle extraction, and gas discharge.[11,12] Fibrous membranes prepared via electrospinning method has wide biomedical applications including bone tissue engineering.[13–15] Material must be able to retain physical stability during preparation and post-transplantation. In order to prevent foreign-body reactions, material must be free of any monomeric impurities. Final material must be evaluated for biocompatibility, extent of biodegradability, and mechanical resistance in accordance with the intended purpose. Therefore, polymeric materials, synthetic or natural based, are widely studied for bone tissue engineering applications.

Poly(ε-caprolactone) (PCL) is a biodegradable hydrophobic polymer with semi-crystalline properties.[16] It is commonly used in the preparation of scaffolds for bone and cartilage tissue engineering.[17] However, PCL is not bioactive, and studies related to high load-carrying capacity of PCL constructs report insufficient mechanical features.[18,19]

Some formulations of calcium sulfate, calcium phosphates (including β-tricalciumphosphate; β-TCP), and hydroxyapatite are bioactive materials with distinct mechanical properties. β-TCP is a resorbable osteoinductive[20] bone graft material which promotes osteoblast adherence and bony tissue deposit on its surface. It has excellent biocompatibility and has chemical similarity to the minerals in bones.[21] While there are some debates on the bonding mechanism, it has been shown that dense sintered β-TCP directly bonds to bone.[22] The osteoconductive property of β-TCP has also been demonstrated.[23]

In this study, we developed a three-dimensional (3D) multispiral scaffold composed of fibrous electrospun PCL/β-TCP composite membranes and tested its capacity for bone tissue formation. Tightly interwoven polymer/bioceramic composite scaffold provided mechanical resistance due

[a)]Electronic mail: elcin@ankara.edu.tr

to its fibrous structure. *In vitro* osteogenic potential of this biomimetic scaffold was evaluated using rat bone marrow mesenchymal stem cells (rBM-MSCs) for 4 weeks. In addition, the extent of ossification on the cell-laden multispiral scaffold was examined ectopically in the epigastric groin fascia of Wistar rats for 6 months.

II. EXPERIMENT

A. Cell isolation and culture

Bone marrow mesenchymal stem cells were isolated from the femurs of Wistar rats (275 ± 25 g) using a well-established technique.[24] Protocols with animals were carried out according to the standards of international regulations. Femurs were aseptically excised and the epiphyses were removed. Then, bone marrow cells were extracted by using alpha-minimum essential medium (α-MEM; Hyclone, Logan, UT, USA) containing 100 U/ml penicillin, 100 μg/ml streptomycin (Pen/Strep; Sigma, St. Louis, MO, USA). Cell suspension was centrifuged (1500 rpm, 10 min), the supernatant was removed, and the process was reiterated. Cells were suspended in α-MEM supplemented with 10% fetal calf serum (FCS; Hyclone) and Pen/Strep, and then transferred to culture flasks. rBM-MSC were cultured at 37 °C under 5% CO_2, 95% air, and 90% humidity with medium changes every other day. Cells were detached at ∼80% confluence using 0.25% trypsin/0.02% ethylenediaminetetraacetic acid (*p*H 7.4; Sigma) and replated at 10^4 cells/cm^2 density. Cells from passages 2 to 4 were used in this study. To confirm the immunophenotype of these cells, flow cytometric analysis was performed with FACSCalibur (BD; Becton Dickinson Biosciences, San Diego, USA) using fluorescein isothiocyanate (FITC)-labeled antibodies against rat antigens CD29, CD44, CD90, and CD45 (BD), after trypsinization and resuspending cells in wash buffer (BD). Nonspecific anti-rat IgG-FITC was used as an isotype control. rBM-MSCs used in this study typically demonstrated a CD29+, CD44+, CD90+, CD34-, and CD45- immunophenotype.

B. Synthesis and characterization of β-TCP

β-tricalcium phosphate was synthesized by using calcium nitrate tetrahydrate [$Ca(NO_3)_2.4H_2O$] and diammonium hydrogen phosphate [$(NH_4)_2HPO_4$] as chemical precursors for calcium and phosphorus, respectively. Ca/P molar ratio was adjusted to 1.5, and the solution was stirred at 25 °C under room temperature. The solution was evaporated; then the product was calcinated at 900 °C. The powder was ground and microparticle aggregates were sieved to a size range <25 μm. Later, β-TCP microparticles were disaggregated in the PCL solution.

Phase identification was made by x-ray diffraction (XRD) analysis (Rigaku D/Max-2200/PC, Tokyo, Japan); copper K_α radiation ($\lambda = 1.5406$ nm) produced at 50 kV and 40 mA; scanned between diffraction angles (2θ) of 5°–75°. Molecular bonding energy of β-TCP microparticles was evaluated by Fourier transform-infrared (FT-IR) (Perkin Elmer-Spectrum 100, Waltham, MA, USA) analysis to verify the structure of the product furthermore. Scanning was performed at wavelengths between 400 and 4000 cm^{-1}. The final β-TCP microparticle size was confirmed by scanning electron microscopy (SEM) (FEI Quanta 200 FEG, Eindhoven, The Netherlands) following electrospinning of fibers. Samples were fixed at 4 °C and 2.5% glutaraldehyde with 0.1 M cacodylate buffer (*p*H 7.4). Fixed samples were coated with a thin layer of gold/palladium and imaged by SEM.

C. Electrospinning of PCL/β-TCP membrane

Poly(ε-caprolactone) (Mw 80 000 Da; Sigma) and β-TCP microparticles were used to prepare the fibrous composite membranes. We prepared the PCL/β-TCP solution by optimizing the ratios of the composite (from 10% to 40% of β-TCP) and the solvent system as follows: dichloromethane/ethanol/tetrahydrofuran/dimethylformamide (4.0:1.0:0.1:0.1). Thirty weight percent β-TCP was found to be optimal among compositions, in terms of maintaining the mechanical stability of the fibrous membranes with the highest β-TCP ratio. Thirty weight percent β-TCP was suspended in solution that contains 10% (w/v) PCL in solvent system. After magnetic stirring, suspension was homogenized by using vortex. β-TCP microparticles were disaggregated by sonication (Fisher FB 15060, Leicestershire, UK), then the resulting composite suspension was transferred into 10 ml syringe. Electrospinning process was performed at 25 kV using a Glassman-DC high-voltage power supply (PS/FC 60P02, High Bridge, NJ, USA), polarizing the gauge connected to a syringe pump, 21G injection nozzle, and a collector plate where fiber was weaved to shape the membrane.

D. Characterization of PCL/β-TCP membrane

Thermal characteristics of the membranes were evaluated by using differential scanning calorimetry (DSC) (Shimadzu DSC-60, Shimadzu Europa, Duisburg, Germany). Samples [unprocessed PCL, bare and 30% β-TCP-containing electrospun PCL (10% w/v)] were heated from 25 to 550 °C at 15 °C/min under nitrogen atmosphere by using aluminum cells. Change in thermal response after electrospinning was evaluated. The average molecular weight of the PCL, which serves as the reinforcement component, was determined by gel permeation chromatography (GPC). Electrospun PCL membrane and unprocessed PCL were dissolved in mobile phase tetrahydofuran and then loaded to the Agilent 1100 GPC device (Santa Clara, CA, USA). Polystyrene was used as the standard to draw calibration curve.

E. Multispiral scaffold construction and characterization

Electrospun composite membranes were cut in appropriate size. Then, membranes were winded up around a stainless steel wire (ø: 350 μm) into spirals of ∼0.7 mm diameter and ∼6 mm height. A cylindrical 3D scaffold with 5 mm diameter and 6 mm height was obtained by assembling ∼70 of these spiral structures. A minute amount (10 μl) of PCL

solvent was contacted with the outer surface of each spiral for their assembly. A scheme for the preparation of the multispiral super-structure is presented in Fig. 1.

SEM analysis was performed to confirm multispiral scaffold morphology. Furthermore, the compressive strength of the construct was investigated by Zwick Z250 Universal Testing Device (Ulm, Germany). Deformation curves of the samples were obtained under constant compression load and stable temperature. Structure was loaded at a rate of 2 mm/min after a preload of 0.7 N. Following formulas were used to assess the mechanical testing results:

$$\text{Stress}\,(\sigma) = \text{force}/\text{surface area}\,(\text{N}/\text{mm}^2), \quad (1)$$

$$\text{Strain}\,(\varepsilon) = (\text{b} - \text{b}_\text{o})/\,\text{b}_\text{o}, \quad (2)$$

where b_o is the original length and b is the deformed length.

Mechanical test results were presented as the resistance of the scaffolds to applied force leading to 1 and 4 mm of decrease in construct height.

F. *In vitro* studies

Scaffolds (either in 2D-membrane or 3D-construct form) were sterilized in 90% ethanol overnight prior to cell culture, and ethanol (ACS reagent, ≥99.5%; Sigma) was eluted by washing with sterile phosphate buffered saline (PBS).

2D-membrane culture was performed as follows: Cells from passages 2–4 were seeded on sterilized fibrous membrane at a density of 1.5×10^4 cells/cm^2, cultured in α-MEM supplemented with 10% FCS (both from Hyclone) and Pen/Strep (standard medium; SM), and allowed to proliferate for 7 days in culture.[25] Subsequently, the medium was switched to osteogenic medium (OM) (SM supplemented with 10^{-8} M dexamethasone, 10 mM Na-β-glycerophosphate, and 50 mg/ml ascorbic acid, all from Sigma) and cultured until the designated time point.

3D-multispiral scaffold culture was performed as follows: Cells from passages 2–4 were seeded on sterilized 3D-scaffold at a density of 2.0×10^6 cells/construct and allowed to proliferate in SM for 7 days in culture. Then, the medium was switched to OM, and the culture was continued for up to 4 weeks. Samples were taken at days 7, 14, and 28 (6 samples per time point). Undifferentiated cellular hybrid structure was used as the control (n = 6).

Cellular constructs were evaluated by histology (using von Kossa and Alizarin red-S stainings) following standard methods.[26] SEM was employed to examine the adhesion, proliferation, and distribution of the cells seeded both on 2D-membrane and multispiral construct. Cellular constructs were washed with PBS and fixed in 2.5% glutaraldehyde in sodium cacodylate buffer overnight at 4 °C. The samples were dehydrated in a series of graded ethanol solutions (60% to 100%) and air-dried at room temperature. The constructs were sputter coated with gold/palladium and analyzed under a scanning electron microscope (FEI Quanta 200 FEG) with an Everhart–Thornley Detector, at 10–20 kV.

Biochemical assays were performed on media specimens collected at days 7, 14, 21, and 28. Increase in alkaline phosphatase activity in the culture medium was quantified by using QuantiChrom Alkaline Phosphatase Assay Kit.[27] The assay is based on the colorimetric determination of yellow colored p-nitrophenol phosphate that is hydrolyzed by

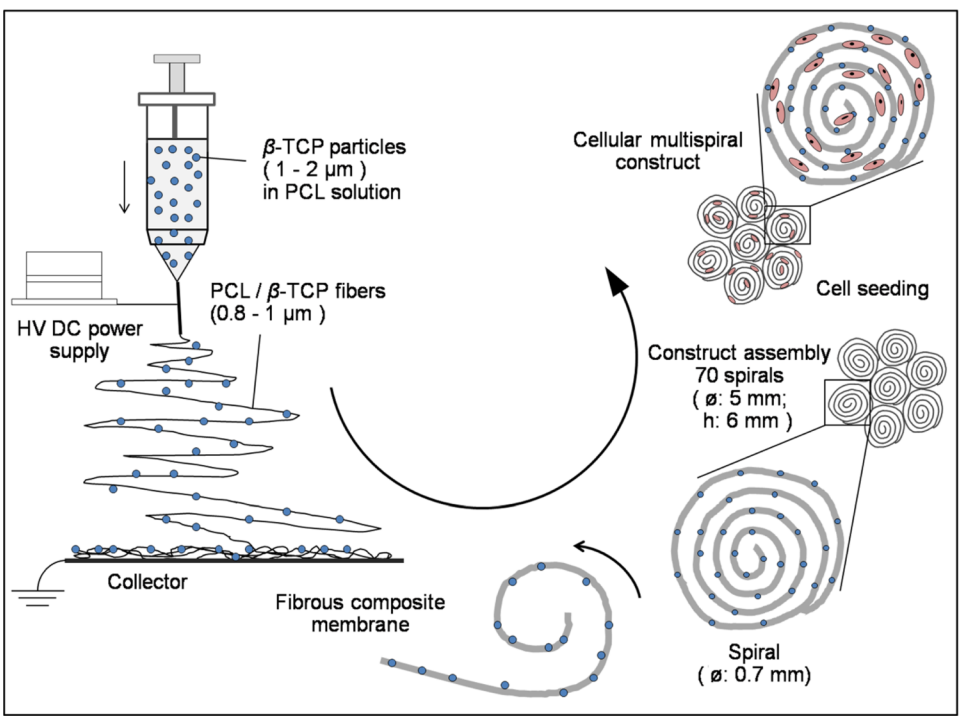


FIG. 1. (Color online) Scheme for the preparation of PCL/β-TCP multispiral super-structure (not drawn to scale).

alkaline phosphatase (ALP), at a wavelength of 405 nm. Spectrophotometric measurements were performed by a SpectraMax M2 model (Molecular Devices, Sunnyvale, CA, USA) microplate reader.

MTT [3-(4,5-dimethylthiazol-2-yl)-2,5-diphenyl tetrazolium bromide]-based assay (Sigma) was used to quantitatively evaluate cell viability, in terms of mitochondrial dehydrogenase activity of the cells. 100 μl of MTT solution (5 mg/ml) was added to 400 μl α-MEM containing the construct and incubated for 4 h at 37 °C and 5% CO_2. MTT taken up by the cells and reduced to the insoluble purple formazan was dissolved in 0.1 N HCl in isopropanol. The absorbances of the samples were measured by a microplate reader at 570 nm wavelength.

G. *In vivo* studies

The ability of rBM-MSCs-containing multispiral PCL/β-TCP constructs to stimulate ectopic bone formation was evaluated in a subcutaneous rat model. Sixteen adult Wistar strain rats (eight females and eight males) weighing 200–250 g at the time of implantation were used. All experimental protocols involving animals were carried out according to the standards of international regulations. 3D-cellular multispiral constructs were ectopically transplanted to the subjects (four rats per time point).[28] Briefly, under anesthesia, 3–4 cm long incisions were made through the skin at the left and right epigastric groin fascia of the subjects. The scaffolds were inserted into the proximal opening of the vascular channel network, cells-containing construct on the right and the cell-free (control) construct on the left groin pockets, and then the incisions were closed in layers. Constructs were explanted at days 7, 14, and 28, and at the 6th month post-transplantation. Animals were sacrificed after the determined period and explants were fixed for 10 min in 2.5% glutaraldehyde solution (in 0.1 M potassium phosphate buffer; *p*H 7.4) and then incubated for 30 min in 15% sucrose solution.[29] The samples were frozen at −80 °C after placing in tissue freezing medium (Tissue-Tek, Sakura Finetek, Zoeterwoude, The Netherlands) for 30 min. Samples were sectioned at 5 μm thickness using a cryotome (Leica CM 1900, Wetzlar, Germany), then mounted on positively charged slides, and stained with von Kossa and Alizarin Red-S (AR-S) for histological analyses. Six-months explant was examined by computed tomography (CT), in order to document the formation of new bone tissue in the ectopic region via calcification. CT scans (Siemens, München, Germany) were performed by applying 130 kV potential, 60 mAs electrical charge, with 1 mm width and 0.5 mm intervals. Cell-scaffold interactions and scaffold integrity were also observed by confocal laser scanning microscope (Leica TCS SP8, Wetzlar, Germany).

H. Statistics

All quantitative results are reported as the mean ± standard deviation for triplicate samples unless otherwise described. Statistical analysis was carried out using the unpaired Student's t test. A value of $P \leq 0.05$ was considered to be statistically significant.

III. RESULTS AND DISCUSSION

Biodegradable polymer-bioceramic composites are commonly preferred for developing bone tissue engineering scaffolds owing to their dual biological and mechanical properties. In addition, bone has mechanical attributes that span from nanoscale to macroscopic dimensions. The proposed structure must behave at multiple length scales, in order to achieve a functional integrity. For ideal bone regeneration, pores of the scaffold must be interconnected, in order to allow material flow between cells.[10] The interface between cell and the scaffold directly influences the viability of seeded cells. Additionally, scaffold provides support for cells that migrate in from the host tissue. Adequate perfusion ensures transportation of gases, nutrients, and metabolic wastes and is a fundamental function for maintaining viability of cell on tissue graft.[8]

One of the aims of the presented study is to develop a 3D multispiral scaffold composed of fibrous electrospun PCL/β-TCP composite membranes. We formed the spiral structures by winding-up fiber composite membranes. Later, we have put spiral structures together, in order to attain structural stability on macroscopic length scale for 3D scaffolds. Each channel constitutes of a 3D scaffold that has a volute structure and thus increases the surface area where cells can adhere and proliferate. The spirals are structurally stable forms successfully allowing the transition from 2D to 3D and from micro to macro.

A. β-TCP and PCL/β-TCP electrospinning

We performed several analyses and evaluations to measure the potentials of the biomimetic PCL/β-TCP multispiral construct. β-TCP powder was first analyzed by XRD, which is presented in Fig. 2(a). The data were consistent with the β-TCP reference, demonstrating crystalline phases of the samples. Specific 2θ angle was observed at 31. FT-IR spectra also confirmed the β-TCP structure,[30] organic bonds between the phosphate and oxygen were confirmed by peaks at 1315–1180 cm^{-1} for P=O and 1100–1050 cm^{-1} for P–O [Fig. 2(b)].

2D poly(ε-caprolactone)/β-TCP fibrous composite membranes were produced by electrospinning; a concept previously explored by Bianco *et al.*[31] In order to ensure a homogeneous dispersion of β-TCP microparticles, prior to electrospinning, we applied magnetic stirring, vortex, and sonication to the polymer-ceramic suspension. Resulting membranes were characterized by differential scanning calorimetry and GPC and compared with each other [Figs. 2(c)–2(e)]. DSC curves of unprocessed PCL [Fig. 2(c)], electrospun PCL [Fig. 2(d)], and electrospun PCL/β-TCP composite membrane [Fig. 2(e)] were compared. We observed a narrowing on the first endothermic curves, and the second endothermic curves gradually disappeared [Figs. 2(c)–2(e)]. GPC analysis of unprocessed and electrospun PCL did not

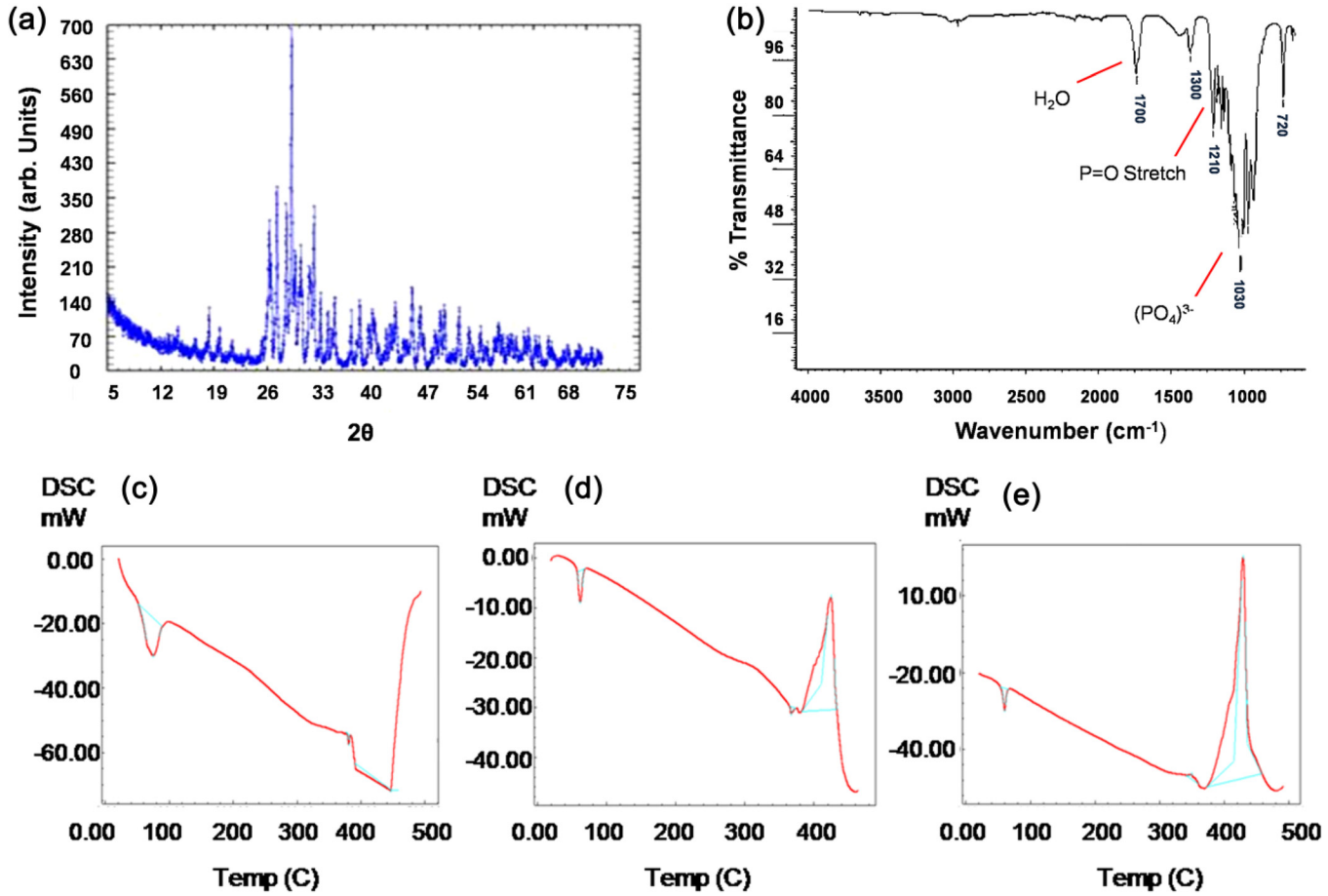


FIG. 2. (Color online) Characterization of the synthesized β-TCP powder: (a) x-ray diffraction pattern demonstrating crystalline phases with the specific 2θ angle at 31; (b) FT-IR results confirm the organic bonds between phosphate and oxygen. Differential scanning calorimetry curves of (c) unprocessed PCL, (d) electrospun PCL, and (e) electrospun PCL/β-TCP composite.

show any significant change in the average molecular weight (Mw/Mn 80 000) of the polymer (not shown).

The first endothermic curve depicts glass transition temperature of unprocessed PCL in DSC analysis [Fig. 2(c)], which modified into a more Gaussian pattern after the electrospinning process [Fig. 2(d)]. This shows that there is a tendency toward an increase in molecular arrangement. Diminishing of the second endothermic curves in the DSC study possibly indicates an increase in molecular consistency, owing to the blending of β-TCP microparticles into PCL polymer solution. The third peak depicts the ascending of the exothermic curve. This may be explained by the increase in the concentration of atmospheric oxygen by the introduction of β-TCP causing a more energetic reaction.

SEM findings revealed that 2D-electrospun PCL/β-TCP membranes were composed of randomly oriented fibers with a fiber diameter mostly ranging between ∼800 and 1000 nm. The pore size in electrospun PCL/β-TCP membranes was observed to be around 5–10 μm from SEM images; however, they were anticipated to be greater than 10 μm under *in vitro* (hydrated) conditions in which H_2O molecules behave as plasticizers on the amorphous regions of composite scaffolds. The fibrous structure provided high surface-to-volume ratio for the whole scaffold.

Fibrous composite membranes were easily removed from the collector plate. They were either cut into 2D-circular form and tentered by the help of 12- or 24-well plate CellCrown inserts (Sigma-Aldrich) for 2D-cell culture or winded up into spiral form and brought together to assemble the 3D-multispiral constructs for further use.

B. Cell-fibrous membrane interactions

To investigate the cell–material interactions, rBM-MSCs were seeded on the electrospun 2D-membranes adjusted for cell culture and were examined for surface adhesion and proliferation under inverted microscope, and the morphological changes were followed daily through the course of 28 days of culture (not shown). It is clear from SEM findings that the size of the β-TCP microparticles after electrospinning together with PCL is typically ∼1–2 μm [Fig. 3(a)]. This also shows that the cohesive β-TCP microparticles, which tend to gather in clusters could be dispersed following vigorous mixing, sonication, and finally electrospinning at an electric potential difference of 25 kV. SEM images also revealed that rBM-MSCs adhered and spread on the interfaces of the fibrous substrate by using their pseudopods [Fig. 3(b)]. As shown in Figs. 3(c) and 3(d), multiplying fusiform cells

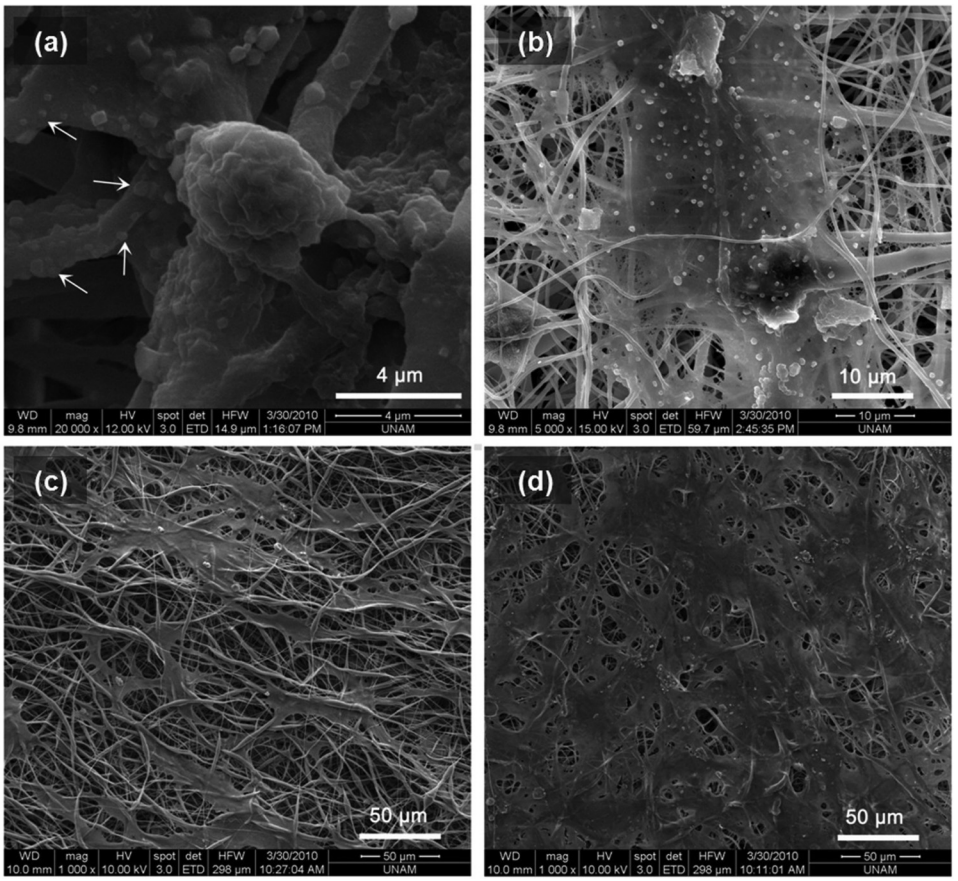


FIG. 3. SEM micrographs demonstrating (a) the homogenous distribution of β-TCP microparticles in the electrospun PCL fibers, (b) cell–membrane interfaces, (c) surface morphology of cell-laden PCL/β-TCP(30%) fibrous membranes at the third day, and (d) at the third week of culture.

populated and completely covered the biomaterial surface and synthesized extracellular matrix (ECM) as the duration of the culture increased.

C. *In vitro* studies with 3D-multispiral construct

In order for a material to be an ideal bone support alternative, porosity of scaffold should be at least 100 μm for structures presenting a suitable mechanical resistance while allowing diffusion of nutrients and transition of metabolic wastes.[32] In addition, cells should disperse homogenously throughout the surface.[33]

When we switched to the osteogenic medium, MSCs with typical fibroblastoid morphology modified into osteogenic cells with strong matrix accumulation. A significant increase in cell expansion and proliferation was also observed in samples collected at designated time points throughout the culture. Cell-free control groups were incubated under the same conditions and time as the cell-laden samples. This way, we were able to compare the effects of cells by excluding any change that is presented by the medium.

Figure 4 demonstrates the inverted images of 3D-multispiral cellular construct at the 7th day of osteogenic culture. Cells could spread throughout the scaffold, on both inner sides of the spirals and on the edges of the junctions [Figs. 4(b) and 4(c)]. As seen in magnified images, gaps and pore surfaces are filled with ECM that were synthesized by the cells, and cell colonies had began to form multilayer tissue like formations [Figs. 4(d)–4(f)]. This can be interpreted as an evidence for osteoconductivity, as the cells migrate to the scaffold and form intercellular structures.

SEM micrographs (Fig. 5) indicate that the spaces both in centers of spiral ($\sim$500 μm) and between fiber layers which constitutes the spirals ($\sim$50–80 μm) of PCL containing β-TCP (30%) have a size range suitable for cell attachment and dispersion. It is also clear from Fig. 5 that rat bone marrow-mesenchymal stem cells could attach and expand on the scaffold by time [compare Fig. 5(b) with Fig. 5(h)]. Cellular extensions accompanied by ECM structures were evident inside the spiral layers and between adjacent spirals [Figs. 5(f) and 5(i)], thus most of the construct channels were filled with cells and ECM after 28 days of osteogenic culture [Fig. 5(h)]. Another observation was that the concentric fibrous layers of the spirals had started to fuse in acellular control scaffolds (but not the cellular scaffolds) under the hydrated osteogenic conditions after 28 days of culture [Fig. 5(g)]. Spaces within channels enable circulation of extracellular metabolites, oxygen, and nutrients by allowing perfusion, and subsequent vascularization and integration of the scaffold in the native tissue. Similarly, Ruckh *et al.*[34] evaluated the interaction of cells with electrospun 2D-PCL fibrous membrane and nontextured control PCL scaffold.

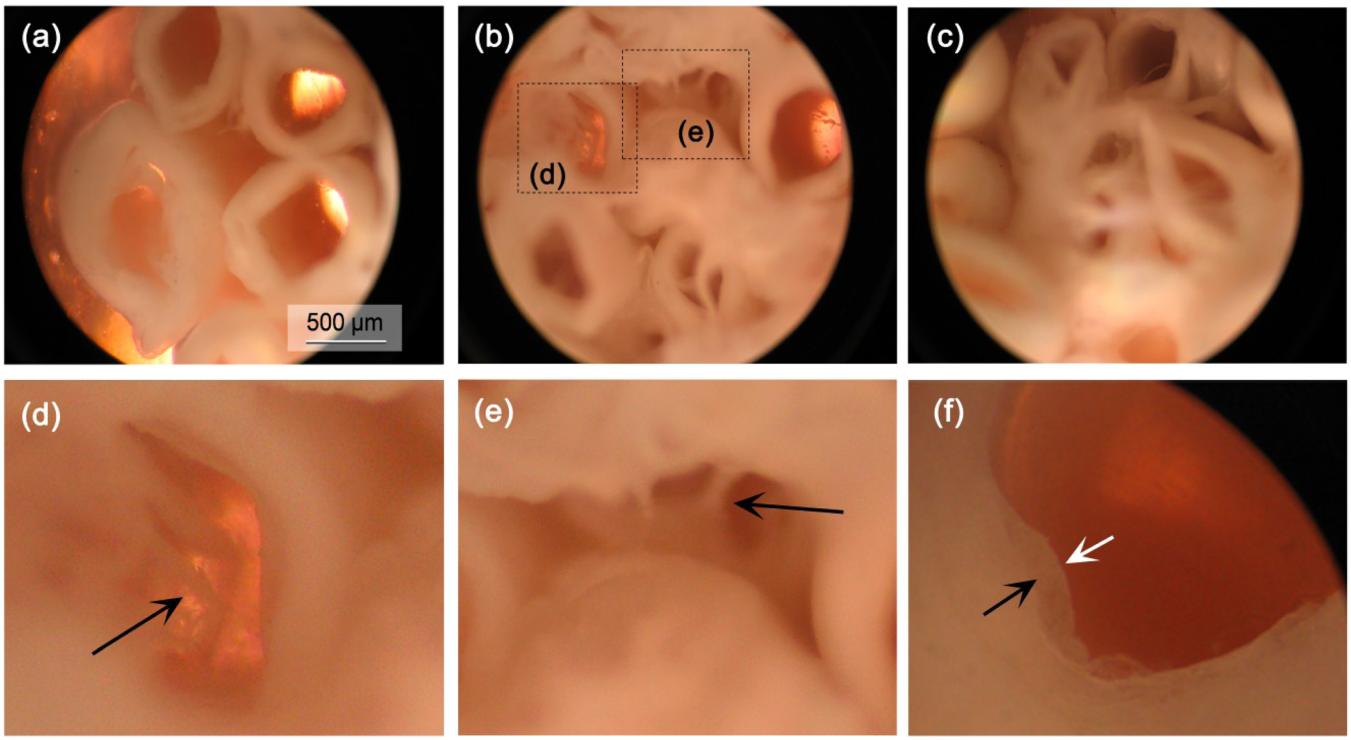


FIG. 4. (Color online) Inversion microscope images of rBM-MSCs on multispiral PCL/β-TCP constructs retrieved at the seventh day of osteogenic culture [(a)–(c)]. Cellular extensions and ECM synthesis are visible in the concentric layers of a spiral (d) and between neighboring spirals (e) in magnified images. Multilayer tissuelike formation is evident along the fibrous membrane surface [(f); arrows].

Results showed that fibrous 2D membranes constitute a better ground for cell adhesion and dispersion in comparison with control. In our study, we incorporated the fibers in order to enhance the dispersive and proliferative capacities of osteogenic cells on the membrane.

It is well known that β-TCP ceramic supports osteoinduction[35,36] and also improves some of the mechanical features of the PCL by forming a composite.[37] The compressive strength of the material was measured and the yield point was calculated as 10 N. Deformation of the structure was observed following the application of forces beyond this magnitude. Table I summarizes the resistance of the dry, wet, and cell-laden scaffolds to applied force leading to 1 and 4 mm decrease in construct height.

Results of *in vitro* histological analyses based on von Kossa and AR-S stainings are presented in Figs. 6(a)–6(f). As known, von Kossa stains phosphate in the presence of acidic material, but it is not sufficient to confirm mineralization by itself. On the other hand, AR-S is used to determine the presence of calcific deposition by osteogenic cells. Findings revealed that cell-laden multispiral constructs were positively stained with both of the markers, with a gradual increase in staining intensity parallel to the osteogenic culture duration. The highest densities of staining were observed on samples from the 28th day cultures [Figs. 6(e) and 6(f)]. These findings confirm that 3D-multispiral composite scaffold structure successfully supported *in vitro* osteogenic differentiation and mineralized matrix production of rBM-MSCs.

In addition to SEM and histological evaluations, we also quantified alkaline phosphate activity to evaluate the *in vitro* biochemical activity of the cells on the scaffold. Alkaline phosphatase activity was found to be 29.544 ± 6.028 U/l for 7th day, 36.896 ± 3.376 U/l for 14th day, 72.235 ± 27.309 U/l for 21st day, and 66.216 ± 20.677 U/l for 28th day [Fig. 6(g)]. Cells at the 21st and 28th days of culture displayed significantly higher ALP activity than the cells at the 7th and 14th days ($P \leq 0.05$).

Overall, ALP activity has the highest value on 21st day of ossification (not on the 28th day). When analyses are evaluated together, this situation can be addressed to the decrease in amounts of biologically available minerals originating from the mineralized ECM covering scaffold surfaces.

MTT tetrazolium reduction assay was applied to evaluate the viability of cells on the multispiral PCL/β-TCP constructs. Findings indicated that the construct was essentially biocompatible, and cells on the construct proliferated by time. The absorbance values were measured as 0.942 ± 0.07 for the 7th day, 1.284 ± 0.081 for the 14th day, 1.458 ± 0.02 for the 21st day, and 1.377 ± 0.023 for the 28th day. Difference between the first (7 days) and the subsequent time points was found to be statistically significant ($P \leq 0.05$). According to the MTT results, a saturation of cell density was observed between days 21 and 28 [Fig. 6(h)], which may be attributed to the formation of a denser calcified extracellular matrix at this time. It is also possible that the dense mineralized ECM have prevented the release of all

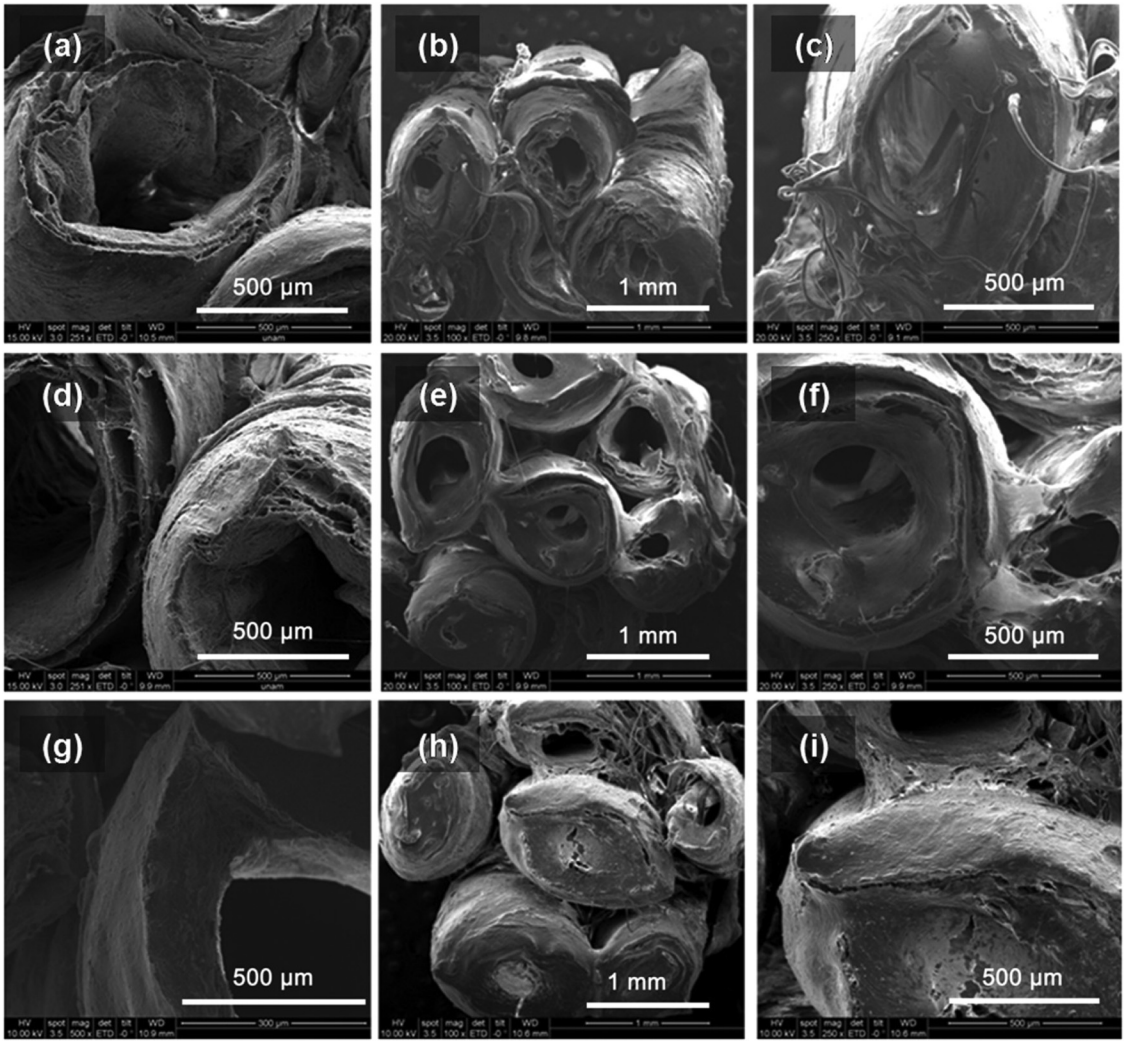


FIG. 5. Representative SEM images of 3D-multispiral PCL/β-TCP constructs from *in vitro* samples retrieved after 7 days [(a)–(c)], 14 days [(d)–(f)], and 28 days [(g)–(i)]. Cell-free scaffolds are shown in (a), (d), and (g). rBM-MSCs attached and expanded on the scaffold by time [(b), (e), and (h)]. As the cells proliferated on the 3D construct, a smoother tissue formation could be observed, thus most of the channels of the structure were filled with cells and the synthesized ECM [(f) and (i)].

the formazan crystals from the entire constructs to the MTT reaction solution among 28th day specimens. Mechanical forces such as sonication and grinding were applied to remove formazan crystal from structure; however, blurriness caused by disintegration of the material in test solution caused inconclusive spectrophotometer readings. The cease of cell proliferation at this time point was attributed to saturation of the entire construct by cell mass and lack of enough metabolites due to high cell concentration.

TABLE I. Mechanical test results.

Sample	F (1 mm) N[a]	F (4 mm) N[b]	E modulus N/mm^2
Dry scaffold	19.66	54.33	34.67
Wet scaffold	20.09	57.47	37.38
Cellular scaffold after 7 days in culture	21.68	55.21	33.53

[a]Applied stress leading to 1 mm of decrease in construct height.
[b]Applied stress leading to 4 mm of decrease in construct height.

D. *In vivo* studies with 3D-multispiral construct

To better investigate the osteogenic potential of the biomimetic multispiral PCL/β-TCP construct, we performed an *in vivo* study and searched for possible ectopic bone tissue-like formation in designated experiment group. Constructs were explanted at days 7, 14, and 28, and at 6 months post-transplantation.

Animal studies indicated that the scaffolds constructed by solution electrospinning did not cause any significant inflammatory reactions, suggesting that they were essentially histocompatible. However, the use of melt electrospinning technique[38] may be an option to eliminate the risk that may arise from potential organic solvent residues.

Histological analysis showed reasonable interaction between the 3D-hybrid structure containing resorbable β-TCP material and the surrounding host tissue. While the construct lacks microenvironmental cues of a nearby regenerating osseous site, it has been demonstrated that a combination of BM-MSC sheet and PCL-calcium phosphate

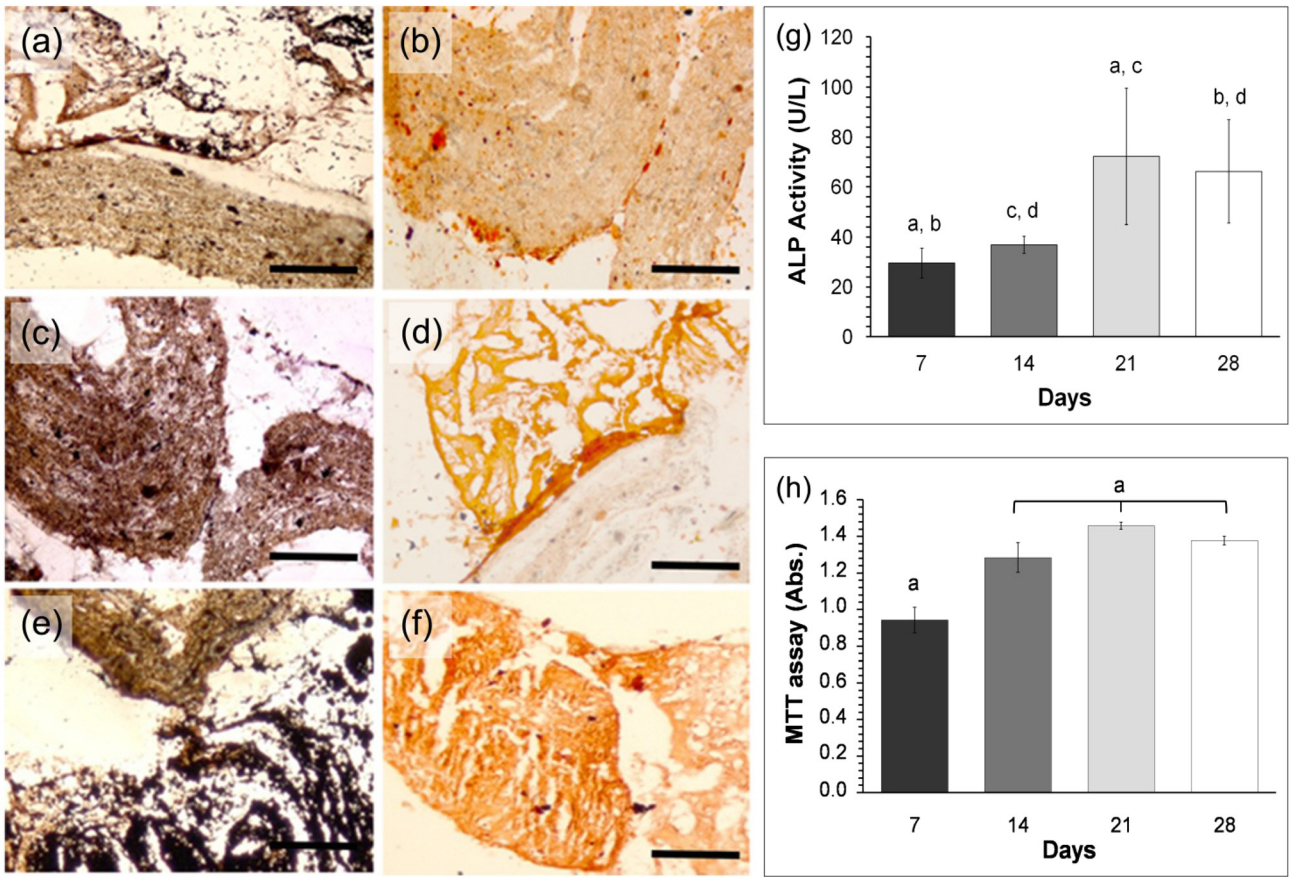


FIG. 6. (Color online) *In vitro* histological findings based on von Kossa [(a), (c), (e)] and AR-S [(b), (d), (f)] stainings of multispiral PCL/β-TCP constructs containing rBM-MSCs cultured under osteogenic culture conditions for 7 days [(a), (b)], 14 days [(c), (d)], and 28 days [(e), (f)]. Scale bars: 100 μm. Biochemical assay performed on the osteogenic *in vitro* cultures of rBM-MSCs seeded on multispiral PCL/β-TCP constructs. (g) Alkaline phosphatase activity of collected culture media at days 7, 14, 21, and 28. (h) MTT tetrazolium reduction assay demonstrating viability of cells on 3D-constructs. Statistically significant differences between the groups: a,a; b,b; c,c; and d,d ($P \leq 0.05$).

composite graft implanted under the skin of nude rats leads to endochondral ossification and intramembranous bone formation.[39] Additionally, it has recently been reported[40] that osteoprogenitors can recruit from bone marrow and home to ectopic site to serve as a cell source for calcium phosphate-induced bone formation. Based on von Kossa and AR-S stainings, it is possible to affirm *in vivo* progressive formation of calcified ECM associated with bonelike tissue at an ectopic site [Figs. 7(a)–7(h)].

Computed tomography [Figs. 7(i) and 7(j)] and confocal laser scanning microscopy [Figs. 7(l) and 7(m)] findings are in line with the histology results. At 6 months post-transplantation, new bonelike tissue could be clearly identified. In Fig. 7(j), CT image exhibits the calcified osteogenic parts, i.e., a part of the spine and the femur, and the calcified zone (in circle), which can be interpreted as ectopic bone. The cellular construct at 6 months post-transplantation was surrounded by a vascular network demonstrating neovascularization at the vicinity of the construct [Fig. 7(k)]. However, further research is needed to quantify the level of neovascularization occurred in transplanted cellular constructs. Cell-scaffold interactions and scaffold integrity were also observed by CLM at the 28th day and 6 months post-transplantation [Figs. 7(l) and 7(m)]. Thus, multispiral PCL/β-TCP constructs were infiltrated by cells/tissue amid lamellar structure. While the new growing bonelike tissue was intact at the end of 6th months, the alteration in the internal structure of the cellular construct resembles an ongoing remodeling process accompanied by scaffold degradation (denoted by histology).

To sum up, the porous composite scaffold was infiltrated with tissue that deposited a calcium-rich matrix during *in vivo* osteogenesis and induced neovascularization at the subcutaneous site. This provides support for structure during regeneration and ensures a favorable environment for replacing natural tissue. Biodegradability of the construct ensures better biological compatibility and creates a leeway for remodeling and osteoinduction, which may improve the ability of scaffold to integrate with the surrounding tissue. Many groups have shown differentiated characteristics from initial mesenchymal identity into bonelike characteristics.[20–23,40] This was confirmed by Alizarin red S and von Kossa stainings, and by CT analysis. Additionally, it was observed that all explants taken during *in vivo* studies integrated with natural tissue and did not cause inflammation.

Predating our results, prominent studies related to bone regeneration also point out that highly porous biomaterials yielded more successful results under *in vivo* conditions.[2,32,41] Percentage of porosity and the size of the pores

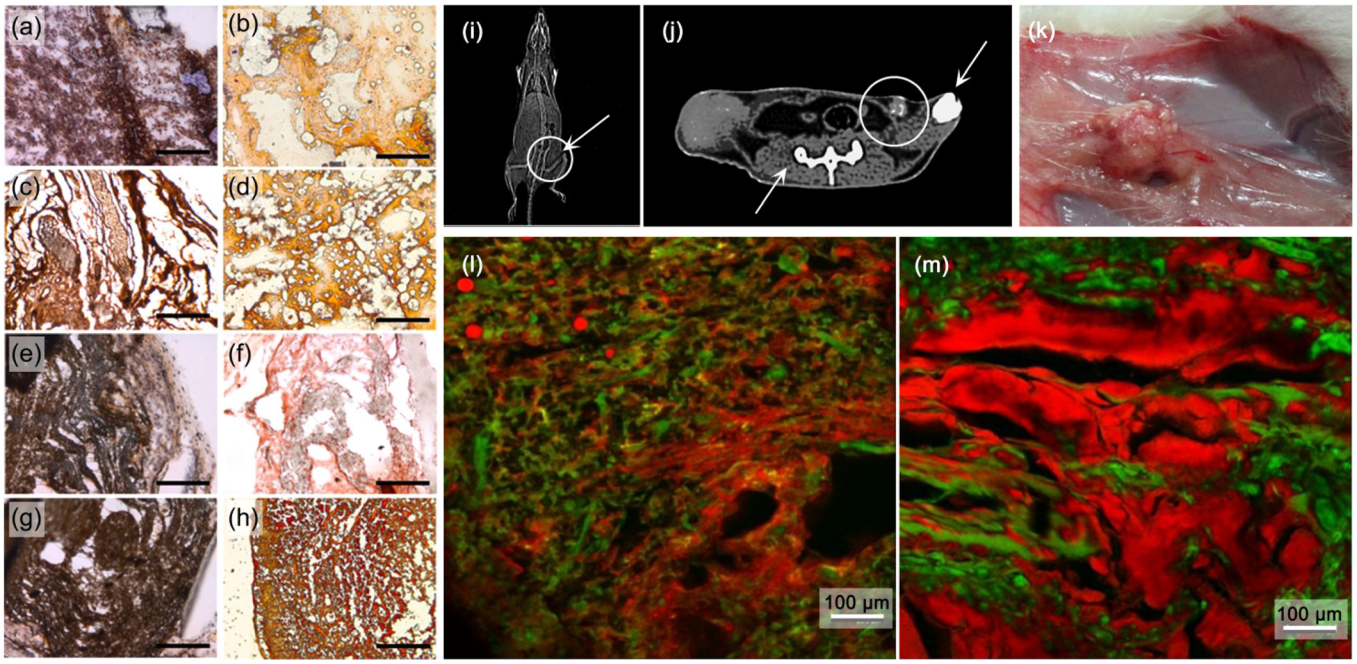


FIG. 7. (Color online) *In vivo* findings of subcutaneously transplanted rBM-MSCs-containing multispiral PCL/β-TCP constructs. Histological findings based on von Kossa [(a), (c), (e), (g)] and AR-S [(b), (d), (f), (h)] stainings of multispiral PCL/β-TCP constructs containing rBM-MSCs transplanted subcutaneously into the epigastric groin fascia of Wistar rats for 7 days [(a), (b)], 14 days [(c), (d)], 28 days [(e), (f)], and 6 months [(g), (h)]. Scale bars: 100 μm. (i) Subcutaneous transplantation site is shown in the general computed tomography view. (j) Ectopic bonelike tissue is visible in the CT image (inside circle) at 6 months post-transplantation (Note the calcified zones corresponding to spine and femur indicated by arrows.) (k) Macroscopic image demonstrates neovascularization at the vicinity of the construct at 6 months post-transplantation. Confocal laser scanning microscopy images taken at the 28th day (l) and 6 months (m) post-transplantation demonstrate infiltration of cells/tissue amid lamellar structure.

are paramount in allowing migration of cells, which is necessary for successful osteoinduction and vascularization. Fiber sizes and correspondingly pore sizes in a construct are essential for cell attachment, proliferation, nutrient, gas and waste transfer, cell–cell communication, and infiltration of the cells into the scaffold. Pore size and fiber density adjustments can also effect *in vivo* bone tissue formation.[32,42] The fibers should allow metabolite flow between pores of bioceramic, support vitality, proliferation, and differentiation, hence constituting areas where cells can easily migrate.[43,44] Also for cells, microenvironment must be familiar and similar to what is natural. Therefore, constructs must be chemically of alike composition to the natural structure. Thus, the β-tricalcium phosphate content mimics the inorganic structure of the bone tissue microenvironment and grants the osteoconductive[23] and osteoinductive[21] capabilities.

IV. CONCLUSIONS

In this study, a 3D-construct was developed from PCL/β-TCP fibrous composite membranes fabricated by electrospinning, then shaping into spirals and assembling into the multispiral form, as a porous bone tissue engineering scaffold to support bone tissue regeneration. β-TCP composite multispiral structures with PCL have mechanical resistance and can contribute in new bone regeneration during *in vitro* and *in vivo* studies. Hybrid cell-scaffold structure implanted in the defected area attains an osteoinductive and osteoconductive character from β-TCP, and structural reinforcement from PCL. Resulting construct has biocompatible, biodegradable composite features all in one. The developed scaffold provides a supportive structure during regeneration and has potential for regenerating bone defects. Further studies are planned to reveal the appropriate timing of transplantation (or *in vivo* conditioning) of the developed construct with the goal to reach the ultimate biomechanical requirements. In addition, more comprehensive studies are planned to reveal the detailed neovascularization potential of this biomimetic construct design.

ACKNOWLEDGMENTS

The support of the Turkish Scientific and Technological Research Council (108M501) is acknowledged. Y.M.E. acknowledges the support of the Turkish Academy of Sciences (TÜBA), Ankara, Turkey.

[1]J. P. Schmitz and J. O. Hollinger, Clin. Orthop. Relat. Res. **205**, 299 (1986).
[2]D. W. Hutmacher, Biomaterials **21**, 2529 (2000).
[3]A. R. Vaccaro *et al.*, Spine J. **2**, 206 (2002).
[4]J. S. Silber, D. G. Anderson, S. D. Daffner, B. T. Brislin, J. M. Leland, A. S. Hilibrand, A. R. Vaccaro, and T. J. Albert, Spine **28**, 134 (2003).
[5]R. Langer and J. P. Vacanti, Science **260**, 920 (1993).
[6]Y. M. Elcin, Adv. Exp. Med. Biol. **553**, 301 (2004).
[7]J. M. Holzwartha and P. X. Ma, Biomaterials **32**, 9622 (2011).
[8]E. L. S. Fong, B. M. Watson, F. K. Kasper, and A. G. Mikos, Adv. Mater. **24**, 4995 (2012).
[9]A. Boccaccio, A. Ballini, C. Pappalettere, D. Tullo, S. Cantore, and A. Desiate, Int. J. Biol. Sci. **7**, 112 (2011).

[10]R. A. Thibault, A. G. Mikos, and F. K. Kasper, Adv. Healthcare Mater. **2**, 13 (2013).
[11]K. Rezwan, Q. Z. Chen, J. J. Blaker, and A. R. Boccaccini, Biomaterials **27**, 3413 (2006).
[12]Y. Zuo, F. Yang, J. G. Wolke, Y. Li, and J. A. Jansen, Acta Biomater. **6**, 1238 (2010).
[13]S. Seker, Y. E. Arslan, and Y. M. Elcin, IEEE Sens. J. **10**, 1342 (2010).
[14]G. C. Ingavle and J. K. Leach, "Advancements in electrospinning of polymeric nanofibrous scaffolds for tissue engineering," Tissue Eng., Part B (published online).
[15]J. Wang and X. Yu, Acta Biomater. **6**, 3004 (2010).
[16]J. O. Iroh, *Poly(epsilon-caprolactone)*, edited by J. E. Mark (Oxford Press, Oxford, 1999), pp. 361–362.
[17]B. Demirdögen, C. E. Bonilla, S. Trujillo, J. E. Perilla, A. E. Elcin, Y. M. Elcin, and J. L. Ribelles, "Silica coating of the pore walls of a microporous polycaprolactone membrane to be used in bone tissue engineering," J. Biomed. Mater. Res., Part A (published online).
[18]K. J. Lowry, K. R. Hamson, L. Bear, Y. B. Peng, R. Calaluce, M. L. Evans, J. O. Anglen, and W. C. Allen, J. Biomed. Mater. Res. A **36**, 536 (1997).
[19]J. C. Reichert, M. A. Woodruff, T. Friis, V. Quent, S. Gronthos, G. N. Duda, M. A. Schütz, and D. W. Hutmacher, J. Tissue Eng. Regener. Med. **4**, 565 (2010).
[20]N. Kondo *et al*., Biomaterials **27**, 4419 (2006).
[21]H. Yuan *et al*., Proc. Natl. Acad. Sci. U.S.A. **107**, 13614 (2010).
[22]M. Neo, T. Nakamura, C. Ohtsuki, T. Kokubo, and T. Yamamuro, J. Biomed. Mater. Res. **27**, 999 (1993).
[23]R. D. Gaasbeek, H. G. Toonen, R. J. Heerwaarden, and P. Buma, Biomaterials **26**, 6713 (2005).
[24]B. Celebi and Y. M. Elcin, J. Proteome Res. **8**, 2164 (2009).
[25]A. Koc, N. Emin, A. E. Elcin, and Y. M. Elcin, J. Bioact. Compat. Polym. **23**, 244 (2008).
[26]Y. M. Elcin, A. E. Elcin, and G. D. Pappas, Tissue Eng. **9**, 1047 (2003).
[27]R. H. Eaton, Clin. Chem. **23**, 2148 (1977).
[28]S. Durkut, A. E. Elcin, and Y. M. Elcin, Artif. Cell, Blood Substitutes, Biotechnol. **34**, 263 (2006).
[29]B. Demirdögen, A. E. Elcin, and Y. M. Elcin, Growth Factors **28**, 426 (2010).
[30]JCPDS file no. 09-169, International Center for Diffraction Data.
[31]A. Bianco, E. D. Federicoa, and I. Cacciottia, Polym. Adv. Technol. **22**, 1832 (2011).
[32]A. G. Mitsak, J. M. Kemppainen, M. T. Harris, and S. J. Hollister, Tissue Eng. Part A **17**, 1831 (2011).
[33]J. R. Jones, L. M. Ehrenfried, and L. L. Hench, Biomaterials **27**, 964 (2006).
[34]T. T. Ruckh, K. Kumar, M. J. Kipper, and K. C. Popat, Acta Biomater. **6**, 2949 (2010).
[35]L. Cheng, F. Ye, R. Yang, X. Lu, Y. Shi, L. Li, H. Fan, and H. Bu, Acta Biomater. **6**, 1569 (2010).
[36]M. P. Ginebra, M. Espanol, E. B. Montufar, R. A. Perez, and G. Mestres, Acta Biomater. **6**, 2863 (2010).
[37]M. Yeo, H. Lee, and G. Kim, Biomacromolecules **12**, 502 (2011).
[38]T. D. Brown, A. Slotosch, L. Thibaudeau, A. Taubenberger, D. Loessner, C. Vaquette, C. Dalton, and P. D. Hutmacher, Biointerphases **7**, 1 (2012).
[39]Y. Zhou, F. Chen, S. T. Ho, M. A. Woodruff, T. M. Lim, and D. W. Hutchmacher, Biomaterials **28**, 814 (2007).
[40]G. Song, P. Habibovic, C. Bao, J. Hu, C. A. van Blitterwijk, H. Yuan, W. Chen, and H. H. Xu, Biomaterials **34**, 2167 (2013).
[41]V. Karageorgiou and D. Kaplan, Biomaterials **26**, 5474 (2005).
[42]M. C. Phipps, W. C. Clem, J. M. Grunda, G. A. Clines, and S. L. Bellis, Biomaterials **33**, 524 (2012).
[43]H. R. R. Ramay and M. Zhang, Biomaterials **25**, 5171 (2004).
[44]S. J. Hollister, Nature Mater. **4**, 518 (2005).